AIAA JOURNAL
Vol. 33, No. 9, September 1995

Panel Dynamic Response to a Reverberant Acoustic Field

H. Nelisse,* O. Beslin,† and J. Nicolas‡
Université de Sherbrooke, Sherbrooke, Québec J1K 2R1, Canada

A novel semianalytical approach based on the integral equation method has been developed to predict the structural response of a panel located in a rigid-walled cavity. This problem is related to the study of the acoustic response of satellite panels with electronic equipment. The main difficulty lies in the treatment of the response of an unbaffled panel, strongly coupled to a high modal density pressure field. A two-indices empty cavity Green's function is used, inspired from electromagnetism. The plate contribution to the sound pressure is obtained by expanding the pressure jump and Green's function on the same basis functions. This approach presents two main advantages: it reduces the size of the linear system to be solved and avoids ill-conditioning problems. This method is found to be quite efficient (10 s per frequency point on a 10 Mflops machine). Results show that the panel responds better at acoustical eigenfrequencies than at its in vacuo modes. The values at which the diffraction phenomena governs the structural and acoustic responses are pointed out in terms of density and flexural rigidity. Finally, the formulation allows the quantification of differences between light and heavy fluid environments.

Nomenclature

b_{nm}	= deflection related unknown coefficients
c	= sound velocity
D	= flexural rigidity
E_y	= Young's modulus
f, ω	= driving frequency, driving angular frequency
$\mathcal{H}$	= Hamiltonian functional of the panel
j	= $\sqrt{-1}$
$\boldsymbol{K}$	= panel stiffness matrix
k	= wavenumber
L_x, L_y, L_z	= x, y, z cavity dimensions
l_x, l_y	= x, y panel dimensions
$\boldsymbol{M}$	= panel mass matrix
N_x^{ac}, N_y^{ac}	= number of acoustic modes in the x and y directions
N_x^p, N_y^p	= number of in vacuo modes in the x and y directions
N_{tu}	= normalization constant for function ψ_{tu}
$\boldsymbol{n}_e$	= rigid wall normal unit vector
$\boldsymbol{n}_p$	= panel normal unit vector
$\boldsymbol{n}_z$	= normal unit vector in the z direction
P_{plate}	= plate sound pressure contribution
P_{source}	= source sound pressure contribution
$\bar{P}_{tu}$	= sound pressure jump related unknown coefficients
$P(r)$	= sound pressure in the cavity
$\bar{P}(x, y)$	= sound pressure jump across the panel
$\boldsymbol{S}$	= basis change matrix
S_e	= rigid wall surface
S_p	= panel surface
S_s	= source surface (piston)
S_T	= surface of the xy section of cavity
$\boldsymbol{S}^\dagger$	= S matrix transpose
V	= cavity volume
$V_a(x, y)$	= acoustic velocity in the $z = z_p$ plane
V_s	= source velocity amplitude
$w(x, y)$	= panel deflection
$\boldsymbol{Z}$	= plate operator
z_p	= z position of the panel
δ	= Kronecker delta
η_a	= fluid damping coefficient (modal damping)
η_s	= structural damping coefficient (modal damping)
ν	= Poisson coefficient
ρ	= fluid density
ρ_s	= mass per unit area of the panel
ρ_v	= mass per unit volume of the panel
$\phi_{nm}(x, y)$	= in vacuo mode of the panel
$\psi_{tu}(x, y)$	= acoustic basis function

I. Introduction

IT is well known in the aerospace industry that the acoustic pressure levels generated by the launch vehicle engines are extremely high. They are responsible for the high levels of acoustic excitation on the different structural components. This strong acoustic pressure excites the secondary spacecraft structures, such as solar panels, communication reflectors, payload panels, and so on. Even though the payloads are designed to maximize the acoustic transmission loss, the satellite and its components are still subject to very high levels of acoustic excitation. This excitation leads to elevated dynamic responses (accelerations) which have to be taken into account by payload designers to circumvent equipment damages. In order to launch proof their product, satellites manufacturers submit their major structural subsystems to standards tests in a reverberant chamber. Some of these major structural subsystems are made up of panels. Such a panel is hung in a large reverberant room and immersed in a diffuse acoustic field. The acoustic pressure (in a one-third octave band) is spatially constant.[1–4] The excitation spectrum and levels are specified, and the structure acceleration levels are measured. These tests lead to a vibroacoustical problem that presents many interesting challenges: 1) the panel is unbaffled, 2) the panel is excited on both sides by an acoustic field, 3) the coupling between the panel and the fluid has to be treated rigorously in order to obtain the pressure jump function across the panel, and 4) the proposed formulation must take into account the pressure of an extremely high modal density in the cavity, even at low frequencies. In other words, even if the field is initially diffuse, the simplifying hypotheses usually found in these types of problems are not admissible.

In the literature, when predicting the effect of an unbaffled structure on an acoustic field, a first approximation is made by assuming that this structure is motionless, leading to diffraction theories. The diffraction of acoustic waves by simple structures, such as rectangular plates, circular disks, and apertures in a baffle, has been studied analytically, numerically, and experimentally by many authors.[5–10] For a flexible structure, even if it has a simple geometry, not many analytical or numerical studies have been conducted. The fact that the structure is unbaffled and acoustically excited tends to complicate the problem since the fluid-structure coupling cannot be neglected. Statistical energy analysis (SEA) approximations are used for the prediction of the high-frequency response,[11–13] whereas, for low and medium frequencies, numerical approaches based

Received Aug. 27, 1994; revision received Feb. 10, 1995; accepted for publication Feb. 16, 1995.

*Ph.D. Candidate, Mechanical Engineering Department, Groupe d'Acoustique.

†Postdoctoral Research Associate, Mechanical Engineering Department, Groupe d'Acoustique.

‡Professor, Mechanical Engineering Department, Groupe d'Acoustique.

on modal approaches give good results.[14–18] However, these approaches require significant computer resources (storage space and CPU time) for a simple configuration used for parametric analysis.

To obtain efficient computer codes, some semianalytical approaches were attempted. Ouellet et al.[19] studied the behavior of a limp panel in a rigid-walled rectangular cavity. Their formulation uses an integral equation method. They used a modal expansion on the cavity modes to describe the physical quantities of interest. Since the chamber is three dimensional, the number of modes increases rapidly with frequency. Therefore, this method is limited to small cavities and plates. Moreover, the presence of an obstacle implies a discontinuity of the pressure function across its surface. To take care of this discontinuity, the authors suggested using three sets of coefficients in the expansion of the pressure gradient and, then, increasing the size of the linear system of equations.

Beslin[20] avoids the discontinuity problem by using a two-indices Green's function first introduced in electromagnetism[21] and applied in acoustics by Bruneau.[22] Beslin studied the case of a holed panel in a rigid-walled cavity. For this panel configuration, there is no straightforward analytical expression for the in vacuo modes. Thus, the author used an approach based on Hamilton's principle where Beslin expressed the holed plate displacement on a set of basis functions independent of the hole shape and defined by the section of the cavity. This formulation leads to a solution that is nonunique. To remove this nonuniqueness problem, he introduced the notion of "ectoplasm." Ectoplasm is an inconsistent material having negligible mechanical properties compared to those of a real plate. It allows the extention of a structure initially defined over a noncanonical domain to a canonical domain and then solves the problem by using a functional basis defined over the canonical domain. This technique can be used to simulate an unbaffled free panel. However, care must be taken in the choice of numerical values of the ectoplasm properties to avoid numerical ill conditioning. For a large cavity, the linear system to solve tends to become quite large since the basis functions are defined over the entire section S_T of the cavity, and so more basis functions must be taken.

In this paper, we present a semianalytical formulation to predict the behavior of an unbaffled plate in a rigid-walled rectangular cavity excited by an acoustical source. This new approach includes several interesting features: 1) the panel is flexible and unbaffled, 2) the excitation on the panel is an acoustic diffuse field rigorously treated with a modal decomposition, 3) the fluid-structure coupling is introduced exactly and allows treatment of light and heavy fluids, and 4) the method is fast enough to allow parametric analysis, a necessary condition for aerospace applications. Our formulation is based, like that of Ouellet et al.,[19] on an integral equation method. The acoustic pressure is expressed using a pressure jump function. The coupling between the fluid and the structure is introduced exactly with this pressure jump function and in the velocity continuity relation at the surface of the panel. A two-indices Green's function[22] is used to express the pressure and the pressure jump functions whereas modal expansion on in vacuo modes is used for the plate deflection. Judicious choice of the integration domain for the basis functions allows one to write a system of linear equations. The pressure jump across the surface and the panel deflection are then obtained with standard linear algebra techniques. Since the two-indices Green's function is used and the in-vacuo modes are defined by the surface of the panel, the formulation becomes a lot faster than those of Ouellet et al.[19] and Beslin.[20]

This paper is divided in three parts. The first part presents an overview of the integral equation formulation dedicated to this problem. In the second part, a novel semianalytical formulation using the two-indices Green's function and the expansion of pressure jump and deflection of the plate is presented. Finally, the third part presents some numerical results, such as the importance of the fluid-structure coupling and the conditions (in mechanical terms) for which the diffraction is the governing phenomena.

II. Integral Equations

A. Geometrical Considerations

A rigid-walled rectangular room (dimensions $L_x \times L_y \times L_z$) containing a thin panel of dimensions $l_x \times l_y$ is considered, as shown in Fig. 1. The cavity can be excited by a vibrating surface S_s lying in the $z = 0$ plane. The wall surfaces (excluding S_s) are S_e, the panel surface is S_p, and the interior volume (excluding S_p) is V. This configuration simulates a satellite panel submitted to acoustic excitation tests in a reverberant chamber.

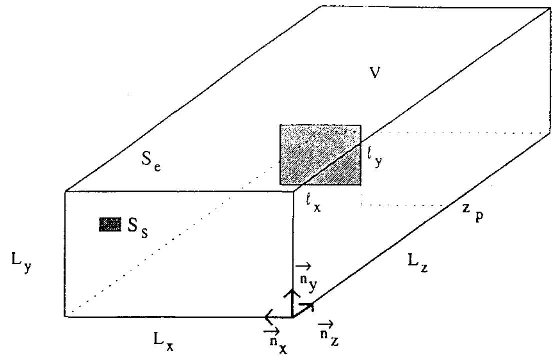

Fig. 1 General representation of a rectangular cavity containing a plate of surface S_p excited by a piston of surface S_s.

B. Formulation for the Acoustic Pressure

The pressure field $P(r)$ must satisfy the following Helmholtz equation and boundary conditions:

$$\nabla_r^2 P(r) + k^2 P(r) = 0 \tag{1}$$

in V, and

$$\begin{cases} \nabla P(r) \cdot n_e = 0, & \text{Neuman condition on } S_e \\ \nabla P(r) \cdot n_s = j\omega\rho V_s & \text{on } S_s \end{cases} \tag{2}$$

Also, k is the wave number related to the piston driving frequency ω by

$$k^2 = \frac{\omega^2}{c^2(1 + j\eta_a)} \tag{3}$$

where η_a is the acoustic damping factor, which includes losses in the fluid. The piston normal velocity V_s is imposed as a boundary condition on S_s.

Using layer potential theories,[22,23] the pressure field can be expressed as follows:

$$P(r_0) = \int\int_{S_s} G(r, r_0)\nabla_r P(r) \cdot n_s \mathrm{d}S - \int\int_{S_p} \bar{P}(x, y)\nabla_r G(r, r_0) \cdot n_p \mathrm{d}S \tag{4}$$

where $G(r, r_0)$, Green's function, satisfies

$$\nabla_r^2 G(r, r_0) + k^2 G(r, r_0) = -\delta(r - r_0) \tag{5}$$

in V, and

$$\nabla G(r, r_0) \cdot n = 0 \tag{6}$$

on $S_e \cup S_s$. The quantity $\bar{P}(x, y)$ is the pressure jump across the surface S_p and is defined by

$$\bar{P}(x, y) = \lim_{\epsilon \to 0}[P(x, y, z_p + \epsilon) - P(x, y, z_p - \epsilon)] \tag{7}$$

The pressure jump function $\bar{P}(x, y)$ can be related to the panel normal velocity (or plate deflection). The pressure jump and the panel normal velocity are both unknowns. They can be identified using the equation of motion of the fluid loaded panel and the continuity of the panel and acoustic field velocities on S_p.

III. Semianalytical Resolution

To identify the pressure jump and the plate deflection, Green's function Eqs. (5) and (6) and pressure jump equation (7) can be expanded on a two-dimensional functional basis. The plate deflection can be expanded on in vacuo modes. Then, a linear system of equations can be obtained by considering the equation of the fluid loaded plate motion and the panel and fluid velocities continuity on S_p.

A. Pressure Field

Instead of expanding Green's function on cavity modes, which implies a triple summation, the function is expanded on a set of two-dimensional functions. It reduces the number of summations by one, which is a great improvement for algorithm efficiency. Such an expansion is written, as shown by Bruneau,[22] in the following form:

$$G(\boldsymbol{r}, \boldsymbol{r}_0) = \sum_{tu} g_{tu}(z, z_0)\psi_{tu}(x, y)\psi_{tu}(x_0, y_0) \tag{8}$$

The orthonormal basis functions ψ_{tu} are given by

$$\psi_{tu}(x, y) = \frac{4}{(1+\delta_{t0})(1+\delta_{u0})L_x L_y}\cos\left(\frac{t\pi x}{L_x}\right)\cos\left(\frac{u\pi y}{L_y}\right) \tag{9}$$

and the function $g_{tu}(z, z_0)$ by

$$g_{tu}(z, z_0) = \begin{cases} -\dfrac{\cos[k_{ztu}(L_z - z_0)]\cos(k_{ztu}z)}{k_{ztu}\sin(k_{ztu}L_z)} & \text{if } z \le z_0 \\ -\dfrac{\cos[k_{ztu}(L_z - z)]\cos(k_{ztu}z_0)}{k_{ztu}\sin(k_{ztu}L_z)} & \text{if } z \ge z_0 \end{cases} \tag{10}$$

where

$$k_{ztu}^2 = k^2 - \left[(t\pi/L_x)^2 + (u\pi/L_y)^2\right] \tag{11}$$

With this Green's function, all of the modes along the z axis are implicitly present and faster convergence can be achieved compared to classical three-indices Green's function.[19] Moreover, since g_{tu} is defined in two parts, it takes into account the pressure discontinuity at $z = z_p$. Ouellet et al.[19] and Beslin[20] have explained the problems related to the use of the three-indices Green's function to reproduce the discontinuous pressure function.

1. *Source Contribution*

With Eqs. (2), (4), (8), and (10) one can calculate the contribution of the piston to the sound pressure:

$$P_{\text{source}}(\boldsymbol{r}) = -j\omega\rho\sum_{tu}\frac{V_{tu}\cos[k_{ztu}(L_z - z)]}{k_{ztu}\sin(k_{ztu}L_z)}\psi_{tu}(x, y) \tag{12}$$

The term V_{tu} is obtained from the integration over the piston surface and is given by

$$V_{tu} = V_s \int_{S_s} \mathrm{d}S\, \psi_{tu}(x, y) \tag{13}$$

The contribution of the piston to the pressure, expressed in Eq. (12), is also the expression for the acoustic pressure for the empty room.

2. *Plate Contribution*

To compute the plate contribution to the pressure, the pressure jump function is expanded on the same basis functions previously used for Green's function. This choice of functions for the expansion is one of the key aspects of our formulation since it allows, as we will see, considerable reduction of the size of the system to be solved and avoids ill-conditioning problems. One then writes

$$\bar{P}(x, y) = \sum_{rs}\bar{P}_{rs}\psi_{rs}(x, y) \tag{14}$$

where the $\bar{P}_{rs}$ are unknown coefficients. Inserting Eqs. (8), (9), (10), and (14) in Eq. (4), one gets

$$P_{\text{plate}}(\boldsymbol{r}) = \begin{cases} \displaystyle\sum_{tu}\frac{\sin[k_{ztu}(z_p - L_z)]}{\sin(k_{ztu}L_z)}\bar{P}_{tu}\psi_{tu}(x, y)\cos(k_{ztu}z) & \forall z \le z_p \\ \displaystyle\sum_{tu}\frac{\sin(k_{ztu}z_p)}{\sin(k_{ztu}L_z)}\bar{P}_{tu}\psi_{tu}(x, y)\cos[k_{ztu}(z - L_z)] & \forall z \ge z_p \end{cases} \tag{15}$$

It is to be noted that the pressure jump at $z = z_p$ is taken into account since the pressure field (15) is defined in two parts.

B. Fluid-Structure Coupling

1. *Equation of Motion of the Plate*

The acoustic pressure field is entirely defined by the pressure jump function, as one can see in Eqs. (12) and (15). This pressure jump is due to the presence of the plate. We then have to relate the pressure jump function to the plate deflection w. The equilibrium condition between the two quantities can be written

$$\bar{P}(x, y) = Z[w(x, y)] \quad \forall (x, y) \in S_p \tag{16}$$

where $\boldsymbol{Z}$ is an operator that represents the mechanical behavior of the plate. $\bar{P}(x, y)$ is, in fact, the density of forces acting on the panel. To obtain the operator $\boldsymbol{Z}$ in a matrix form we developed the deflection of the plate on in vacuo modes of the panel. One then can write

$$w(x, y) = \sum_{nm} b_{nm}\phi_{nm}(x, y) \quad \forall (x, y) \in S_p \tag{17}$$

Two types of boundary conditions have been considered for the plate: the guided plate and the simply supported plate. This choice is motivated by the fact that the in vacuo modal shapes ϕ for these boundary conditions are well-known analytically and are given by

$$\phi_{nm}(x, y) = \begin{cases} \dfrac{4}{(1+\delta_{n0})(1+\delta_{m0})l_x l_y}\cos\left(\dfrac{n\pi x}{l_x}\right)\cos\left(\dfrac{m\pi y}{l_y}\right) & \text{guided} \\ \dfrac{4}{l_x l_y}\sin\left(\dfrac{n\pi x}{l_x}\right)\sin\left(\dfrac{m\pi y}{l_y}\right) & \text{simply-supported} \end{cases} \tag{18}$$

The guided plate allows a rigid body translation mode along the z axis. The influence of this mode at low frequencies can be studied by comparison with the simply supported plate which does not allow this mode.

The Appendix shows the calculations for the $\boldsymbol{Z}$ operator for a guided and simply supported plate. Both can be expressed as follows:

$$Z_{nmpq} = -\omega^2 M_{nmpq} + K_{nmpq} \tag{19}$$

The $\boldsymbol{M}$ and $\boldsymbol{K}$ matrices are given in the Appendix.

Using Eq. (14), the fluid loaded plate motion is given by

$$\sum_{nm}\sum_{pq} Z_{nmpq}b_{pq}\phi_{nm}(x, y) = -\sum_{rs}\bar{P}_{rs}\psi_{rs}(x, y) \tag{20}$$

on S_p. Equation (20) represents one part of the fluid-structure coupling. As will be shown in the next section, the other part is given by the fluid and panel velocities continuity.

2. *Velocities Continuity Condition*

At the interface between the panel and the fluid, the panel and acoustic velocities must be equal. This is what we call velocities continuity on S_p. The acoustic velocity V_a in the $z = z_p$ plane can be written

$$V_a(x, y) = -\frac{1}{j\omega\rho}\left.\frac{\partial P}{\partial z}\right|_{z=z_p} \tag{21}$$

Using Eqs. (12) and (15), Eq. (21) can be rewritten

$$V_a(x,y) = \frac{1}{j\omega}\sum_{tu}[Y_{tu}\bar{P}_{tu} - W_{tu}]\psi_{tu}(x,y) \qquad (22)$$

where

$$Y_{tu} = \frac{1}{\rho}k_{ztu}\frac{\sin[k_{ztu}(z_p - L_z)]\sin(k_{ztu}z_p)}{\sin(k_{ztu}L_z)} \qquad (23)$$

$$W_{tu} = j\omega V_{tu}\frac{\sin[k_{ztu}(z_p - L_z)]}{\sin(k_{ztu}L_z)} \qquad (24)$$

Differentiating the panel deflection with respect to time, the velocities continuity reads, after multiplication by $j\omega$,

$$\sum_{tu}[Y_{tu}\bar{P}_{tu} - W_{tu}]\psi_{tu}(x,y) = -\omega^2\sum_{nm}b_{nm}\phi_{nm}(x,y) \qquad (25)$$

on S_p. Equations (20) and (25) completely define the fluid-structure interaction.

C. System of Linear Equations

The pressure jump (14) to be identified is defined over the S_T domain. Equation (20) relates the pressure jump and the panel velocity on the S_p domain. On the complementary domain $S_T - S_p$, the pressure jump must vanish since there is no obstacle. Thus, multiplying both sides of Eq. (20) by the basis function ψ_{tu} and integrating over S_T one gets

$$\sum_{rs}\bar{P}_{rs}\int_{S_T}\mathrm{d}S\psi_{rs}\psi_{tu} = -\sum_{nm}\sum_{pq}Z_{nmpq}b_{pq} \times \int_{S_p}\mathrm{d}S\,\phi_{nm}\psi_{tu} + \int_{S_T - S_P}0\,\mathrm{d}S \qquad (26)$$

A transform matrix S from the ψ to the ϕ basis can be defined:

$$S_{nmtu} = \int_{S_P}\mathrm{d}S\ \phi_{nm}\psi_{tu} \qquad (27)$$

Then, Eq. (26) can be rewritten, since ψ is an orthonormal basis,

$$\bar{P}_{tu} = -\sum_{nm}\sum_{pq}S^{\dagger}_{tunm}Z_{nmpq}b_{pq} \qquad (28)$$

Using the same approach, multiplying relation (25) by ϕ_{pq} and integrating over S_p, one can write

$$\sum_{rs}S_{pqrs}[Y_{rs}\bar{P}_{rs} - W_{rs}] = -\omega^2\sum_{nm}b_{nm}I_{nmpq} \qquad (29)$$

with I, the unit matrix.

Inserting Eq. (28) in Eq. (29), one obtains the following linear system of equations to solve:

$$[S\,Y\,S^{\dagger}\,Z - \omega^2\,I][b] = [-S\,W] \qquad (30)$$

This system is well conditioned and easily resolved with classical algorithms. It has to be solved for each frequency step.

Advantages related to this formulation are that all of the physical quantities can be obtained with just the b_{nm} set; it also reduces the computation time. The plate velocity and the acceleration can be obtained from Eq. (17), the pressure jump can be obtained from Eq. (28), and the sound pressure is given by Eqs. (12) and (15). In their formulations, Ouellet et al.[19] and Beslin[20] had to solve a system containing more than one set of coefficients. The formulation developed here only requires one set of coefficients. This is due to 1) a judicious choice of functions and domains of integration and 2) the use of orthogonal basis functions. This last point is a determinant advantage in favor of this formulation since it allowed us to obtain the unit matrices in the fluid-structure coupling equations.

IV. Numerical Results

A. Change of Basis Matrix S: Convergence of the Method

The S matrix is the transform matrix from the ψ (acoustic) basis to the ϕ (structural) basis whereas $S^{\dagger}$ is the transform matrix from ψ to ϕ. To ensure convergence of the method, the number of acoustic and structural basis functions must be determined properly. If it is assumed that enough in vacuo modes for the plate are used so that the last modes have less weight in the modal expansions, one can state the following criterion: the smallest $x(y)$ wavelength of the acoustic basis functions must be less or equal to the smallest $x(y)$ wavelength of the in vacuo modes. Mathematically, for cosine or sine functions and modes, this condition can be expressed as

$$N_x^{ac}/L_x \geq N_x^p/l_x$$
$$N_y^{ac}/L_y \geq N_y^p/l_y \qquad (31)$$

In other words, the acoustic basis must have greater or equal "definition" than the definition of the structural basis.

One can distinguish three zones for our criterion: the subcritical where the criterion is not met, the critical [equal sign in Eq. (31)], and the supercritical cases. As an example, if we have a 2×2 m panel, a 4×6 m section for the cavity and if we choose 10×10 (100) modes for the panel, we will have to take at least 20×30 (600) acoustic functions to ensure good accuracy, a value that represents the critical limit. Then, it becomes clear that the number of acoustic functions increases rapidly with the x–y dimensions of the room.

Figure 2 illustrates this effect. A $0.7 \times 0.5\,\mathrm{m}^2$ simply supported plate has been placed in the center of a $2.6 \times 2.0 \times 2.0\,\mathrm{m}^3$ room excited at 90 Hz. The absolute value of the pressure jump is represented vs the x position in the cavity (the y position is fixed at a value that stands between the y limits of the plate). In the x direction, the plate lies between 0.95 m and 1.65 m. For the critical and supercritical case, the pressure jump vanishes, as expected, for the $S_T - S_p$ domain. However, for a subcritical number of acoustic functions (20×20 acoustic functions for 10×10 structural modes), the sound pressure jump presents an oscillatory behavior that is inconsistent with the physics of the problem. The wavelength of this oscillation corresponds to the smallest x wavelength of the ψ basis set. It could be thought the Fig. 2 does not directly demonstrate that the pressure jump has converged to an accurate solution for the physical problem under investigation. However, it has been verified that, substituting this pressure jump back into Eq. (25), acoustical and panel velocities are actually equal. As will be shown in the next sections, panel velocity levels obtained using this method are meaningful, and so it can be assumed that the pressure jump presented in Fig. 2 corresponds to an expected physical result.

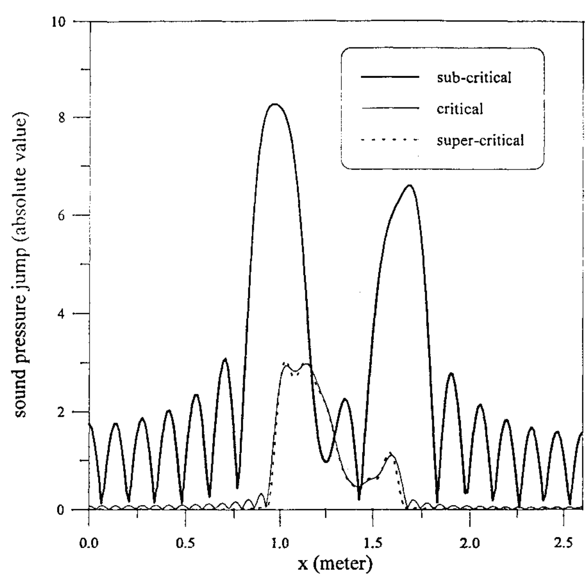

Fig. 2 Absolute value of the sound pressure jump level as a function of the x position in the cavity (y position fixed) for three different numbers of acoustic basis functions.

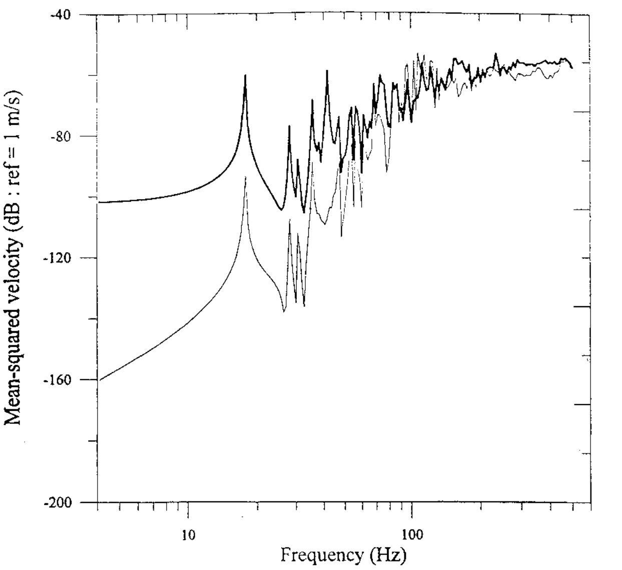

Fig. 3 Mean-squared deflection as a function of the frequency for a sandwich plate of 2.0 × 1.5 m^2; cavity is 8.9 × 6.9 × 9.75 m^3; thick line is the guided boundary condition and thin line is the simply supported case.

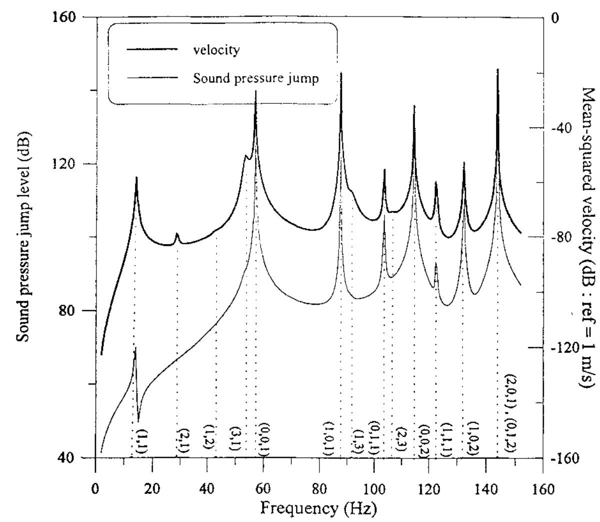

Fig. 4 Mean-squared sound pressure jump and velocity levels as a function of the frequency for a 0.7 × 0.5 m^2 simply supported aluminum plate; cavity is 2.6 × 2.0 × 3.0 m^3; left axis refers to the sound pressure jump, right axis to the velocity; empty cavity acoustic modes are indexed (i, j, k) in vacuo structural modes are indexed (n, m) at the bottom of the graph.

B. Physical Results

1. *Effect of the Boundary Conditions on the Velocity Response*

As mentioned earlier, the formulation developed allows the rapid calculation of a panel response in a room for typical aerospace applications. Curves shown in Fig. 3 present the mean-squared velocity levels for a typical 2.0 × 1.5 m^2 simply supported and guided honeycomb sandwich panel in a large chamber of dimensions 8.0 × 6.9 × 9.75 m^3 as a function of the frequency (the NAE chamber in Ottawa, Canada, is this size and is used for acoustic testing for the aerospace industry). The panels were placed at the $z_p = 3.8$ m position. In the frequency range studied 10,000 points were taken and integrated over the 1/16th octave bands since the number of acoustic modes is very large for this type of room. Each frequency step took about 10 s of CPU time on a 10 Mflops computer; therefore, large quantities of data can be obtained in a relatively short time.

For low frequencies, the guided plate gives higher velocity levels. This was expected since the piston mode is present for such a boundary condition. Moreover, one obtains the well-known flexural behavior at very low frequencies for the simply supported case. For the guided case, a mass-law behavior should be expected at very low frequencies. However, the frequency dependence is driven by the acoustic impedance since the mass per unit area of a honeycomb sandwich panel is low compared to this impedance. For higher frequencies, the two curves tend to merge since the contribution of the piston mode decreases with frequency. Since the number of acoustic modes is important for a large room, frequency integration must be made to obtain reasonable and comprehensive results. Thus, the remainder of this paper is restricted to medium-sized cavities and plates in order to quickly demonstrate some interesting physical features related to our formulation.

2. *Structural Velocity and Pressure Jump Interpretation*

To validate the computer code, the case of a 0.7 × 0.5 m^2 simply supported aluminum panel placed in a 2.6 × 2.0 × 3.0 m^3 cavity has been studied in order to determine the possibility of retrieving the acoustic and structural resonances of the empty cavity and in vacuo panel. The panel has a Young's modulus of 7.1 × 10^{10} Pa, thickness of 1 mm, and a density of 2700 kg/m^3. Figure 4 shows the pressure jump level and the mean-squared velocity level as a function of the frequency in the 2–152-Hz range.

All of the peaks have been identified and correspond to the (i, j, k) empty cavity and (n, m) in vacuo panel modes. At the bottom of the figure, the corresponding modes have been identified for each peak. It is interesting to see that the plate response is more prominent for acoustical modes than for its own in vacuo modes. Moreover, the pressure jump seems unaffected by the velocity resonances [see, for example, the (2, 1) mode] except for the first mode (1, 1). This confirms the importance of the fluid-structure coupling. Nevertheless, not all of the acoustical and structural modes appear in the velocity response. Structural modes for which an integration over the panel surface is zero seem not to contribute above the first acoustical mode frequency. Acoustical modes with no z component also do not contribute.

These results suggest that the panel acts first as a fixed obstacle so that the acoustical response is first driven by diffraction effects. Therefore, if the flexural response of the panel is desired, knowledge of the sound pressure jump (the forces acting on the plate) is not sufficient to completely characterize the response of the plate.

3. *Diffraction as a Governing Phenomenon*

The importance of the diffraction effect becomes clear by looking at Figs. 5a and 5b. In these figures, two 0.7 × 0.5 m^2 simply supported panels have been compared in the 2.6 × 2.0 × 3.0 m^3 cavity at 90 Hz. The first case presents an aluminum plate of 1 mm thickness, denoted "light" on the figure, whereas the second case is a heavy "hypothetical" panel of weight 472 kg ($\rho_v = 27{,}000$ kg/m^3, $E_y = 7.1 \times 10^{10}$ Pa, and thickness = 5 cm). In Fig. 5a the absolute value of the pressure jump is shown as a function of x for a fixed y position. In Fig. 5b, the mean-squared velocity is shown as a function of x where in this case x is lying only on the plate limits. Despite the great difference in mass between the two panels, the sound pressure jump remains approximately unchanged for the two cases whereas the velocity falls dramatically (~90-dB drop). Consequently, it confirms the prior assertion that the diffraction effect is dominant for the acoustical part of the problem, at least for the type of panel studied.

A question must now be answered: For what type of plate is this diffraction effect important? Investigating the sound pressure jump changes while modifying the mechanical properties of the panel (mass and flexural rigidity) brings forth some answers. Figure 6 shows pressure jump level as a function of $\log(\rho_s)$ and $\log(D)$ for the 0.7 × 0.5 m^2 panel in the 2.6 × 2.0 × 3.0 m^3 cavity. The frequency of excitation is 90 Hz. As expected, the pressure jump is low for low-flexural rigidities and masses. For some values of D and ρ_s the sound pressure jump reaches a plateau, after which the level remains unchanged. Five typical cases of plates encountered in the industry have been plotted on the figure: aluminum of 5 mm and 1 cm (1 and 2), steel of 5 mm and 1 cm (3 and 4),

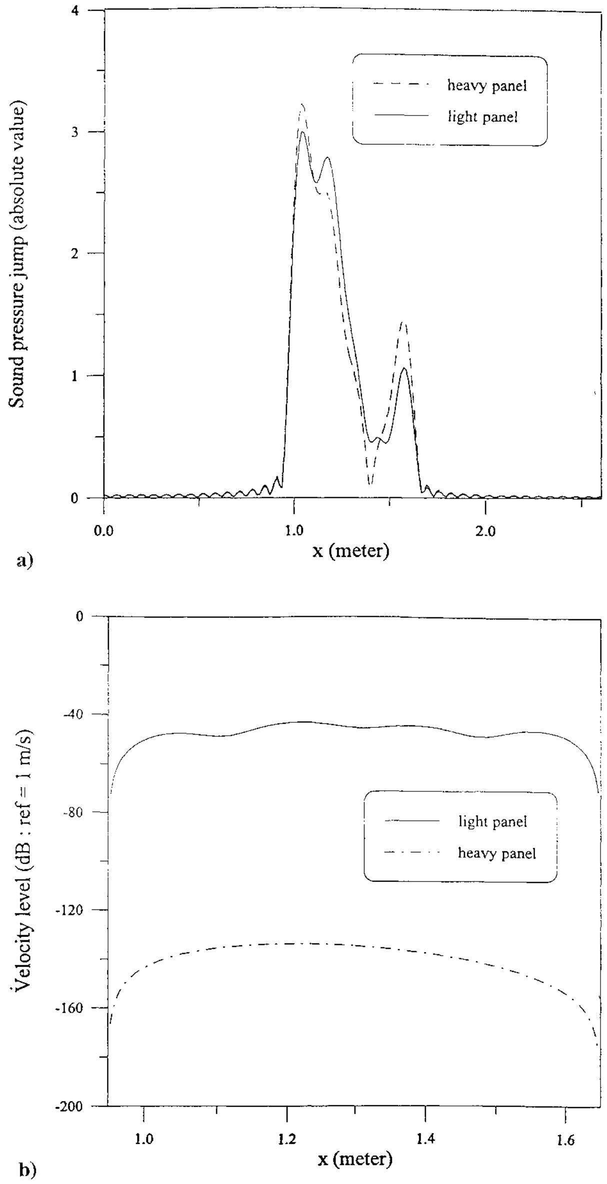

Fig. 5 Comparison of the response of a light and a heavy panel: a) absolute value of the sound pressure jump as a function of the x position in the cavity, y position fixed, and b) deflection level, in dB, as a function of the position x on the panel.

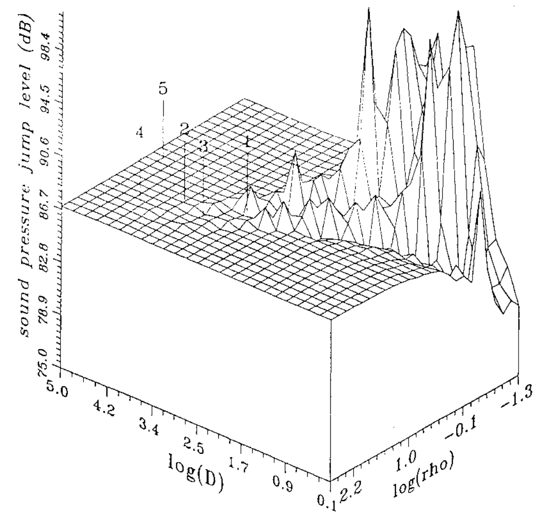

Fig. 6 Mean-squared sound pressure jump level as a function of log(ρ_s) and log(D); panel is 0.7 × 0.5 m^2, cavity is 2.6 × 2.0 × 3.0 m^3 and frequency of excitation is 90 Hz; five values of ρ_s and D are shown for typical panels.

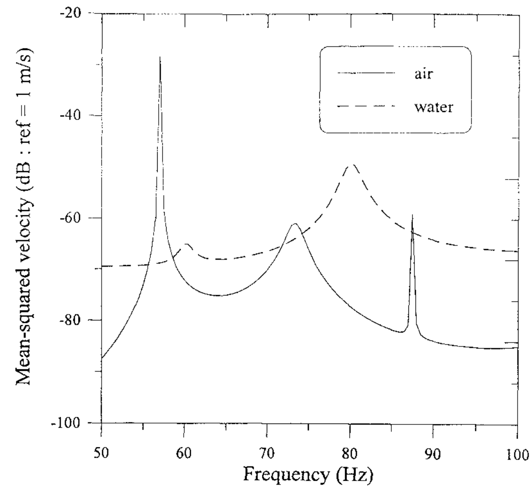

Fig. 7 Mean-squared velocity of a panel immersed in water and in air as a function of the frequency for the 0.7 × 0.5 m^2 simply supported panel and for the 2.6 × 2.0 × 3.0 m^3 cavity.

and a typical sandwich panel (5). One can see that about all of the interesting applications lie in the plateau. This plateau represents, once again, a region where the diffraction effect is the most important. However, such a conclusion can only be made for low frequencies.

4. Fluid-Structure Coupling: Light and Heavy Fluid

Another important aspect of our approach is that the fluid-structure coupling is taken into account without approximation. Figure 7 shows the case of a 0.7 × 0.5 m^2 simply supported aluminum panel of 5 mm thickness positioned at $z_p = 1.8$ m in a 2.6 × 2.0 × 3.0 m^3 cavity. The mean-squared velocity is plotted for the panel immersed in air and in water. The curve for the air shows two narrow peaks which represent the (0, 0, 1) and (1, 0, 1) real acoustic modes. Note that the (1, 0, 0) and (0, 1, 0) modes do not appear since they have no z component. The broad peak represents the first in vacuo mode of the panel (in vacuo calculations give $f_{11} = 74$ Hz). When the cavity is filled with water, the structural peak is shifted toward the low frequencies, in agreement with the well-known added-mass effect. The second peak comes from the second in vacuo mode of the plate, considerably shifted by the fluid (in vacuo calculations give $f_{21} = 149.8$ Hz). No acoustic peaks are present in the water case since the first nonzero frequency mode appears at 246 Hz. Using the same velocity magnitude for the acoustical source, the velocity levels are higher in the water case since the injected energy is higher. Similar results have been obtained for the mean-squared sound pressure-jump levels. These results show that the model can be used to understand and validate experimental studies for the case of a panel immersed in a water tank.

V. Conclusion

Pure diffraction and acoustic radiation (baffled structures) have been investigated for about two decades and are well understood. However, the combination of these two phenomena, for a nonbaffled structure and for a closed volume of fluid, presents many unstudied aspects. The dynamic response of a panel immersed in a diffuse field is not only an open problem with regard to the theoretical formulation and comprehension of physical phenomena, but it is also of technical interest from the point of view of the aerospace industry.

The novel formulation proposed in this study deals with all of the difficulties without approximations and takes the fluid-structure coupling rigorously into account. The main originality in this work lies in the fact that the sound pressure jump is expanded on the same basis functions as the ones used for Green's function, these being especially chosen to be expanded with a set of two indices instead of three, as is done classically. The resulting system of linear equations presents two important advantages: on one hand, the ill-conditioning and convergence problems are solved and, on the other hand, the numerical resolution is fast since it involves only the set of unknown coefficients related to the deflection of the panel. The proposed approach is not limited by the frequency, converges strictly with the use of a simple criterion, facilitates the comprehension of physical phenomena, and is convenient for parametric analysis.

The main points are as follows: 1) One obtains a higher structural response of the panel at acoustic modes than at its own in vacuo modes. Physically, this fact expresses a strong coupling between the fluid and the structure. In practice, it indicates that the experimental characterization of the pressure and sound pressure jump distribution is not sufficient to correctly obtain the dynamic response of the panel. 2) The importance of the diffraction effect, which seems to be the dominant effect on typical panels, is determined. The parametric analysis, as a function of ρ_s and D, brings to light probably for the first time, for which zones the panel acts as if it is rigid and the zones for which this effect is less important. 3) The generality of the model allows a quantification of the difference between the behavior of a panel immersed in a light fluid (air) and a panel immersed in a heavy fluid (water). Future studies will be devoted to the addition of mass and inertia effects on the panel in order to simulate the attachment of electronic equipment and to determine, thanks to the present model, the level of acceleration to which they are submitted.

Appendix: Calculation of Operator Z

The purpose of this calculation is to obtain a matrix form for the operator **Z**. The Hamiltonian functional of a simple panel submited to external forces F_{ext} can be written as

$$\mathcal{H} = \int_{t_1}^{t_2} \int_{S_p} \left[\frac{1}{2}\rho_s(x, y)(\partial_t w)^2 - \frac{D}{2}\left\{ \left(\partial_{xx}^2 w\right)^2 + \left(\partial_{yy}^2 w\right)^2 + 2\nu\partial_{xx}^2 w \partial_{yy}^2 w + 2(1-\nu)\left(\partial_{xy}^2 w\right)^2 \right\} + F_{\text{ext}} w \right] \mathrm{d}S\,\mathrm{d}t \tag{A1}$$

The mass per unit area $\rho_s(x, y)$ is chosen to be space dependent in order to allow the placement or positioning of added masses on the plate. The first term of Eq. (A1) represents the kinetic energy whereas the second is the potential energy. The last term is the energy due to external forces. In the present case of interest, the external force is the sound pressure jump $\tilde{P}$.

If we use the in vacuo modes of the guided or simply supported plate from Eq. (18) to develop the plate deflection w, it is easy to show that the Hamiltonian is given by

$$\mathcal{H} = \mathcal{H}_{\text{kin}} + \mathcal{H}_{\text{pot}} + \mathcal{H}_{\text{ext}}$$

$$= \int_{t_1}^{t_2} \left[\tfrac{1}{2}\dot{b}_{nm} M_{nmpq} \dot{b}_{pq} - \tfrac{1}{2} b_{nm} K_{nmpq} b_{pq} + \tilde{F}_{pq} b_{pq} \right] \mathrm{d}t \tag{A2}$$

The matrices $\boldsymbol{M}$ and $\boldsymbol{K}$ are given by

$$M_{nmpq} = \int_{S_p} \mathrm{d}S \rho_s(x, y) \phi_{nm} \phi_{pq} \tag{A3}$$

$$K_{nmpq} = D\left(k_p^2 + k_q^2\right)^2 \delta_{np} \delta_{mq} \tag{A4}$$

with $k_p = p\pi/l_x$ and $k_q = q\pi/l_y$. $\tilde{F}$ is the so-called generalized force and is written

$$\tilde{F}_{pq} = \int_{S_p} \mathrm{d}S\, F_{\text{ext}}(x, y) \phi_{pq} \tag{A5}$$

By the use of Hamilton's principle, the solution vector $\boldsymbol{b}$ is found to minimize the Hamiltonian given in Eq. (A2). Then, one can write

$$\frac{\partial \mathcal{H}}{\partial b_{nm}} = 0 \qquad \forall\,(n, m) \tag{A6}$$

If an harmonic state is assumed for the time dependence of the deflection, one has $b_{nm}(t) = b_{nm} e^{j\omega t}$. Then, one can easily show that Eq. (A6) gives

$$\sum_{pq} Z_{nmpq} b_{pq} = \tilde{F}_{nm} \tag{A7}$$

where

$$Z_{nmpq} = -\omega^2 M_{nmpq} + K_{nmpq} \tag{A8}$$

Acknowledgments

This work was supported by grants from the National Sciences and Engineering Research Council of Canada (NSERC). The authors would like to thank SPAR aerospace for helpful discussions.

References

[1] Morrow, C. T., "Point-to-Point Correlation of Sound Pressure in Reverberation Chamber," *Journal of Sound and Vibration*, Vol. 16, No. 1, 1971, pp. 29–42.

[2] Waterhouse, R. V., "Statistical Properties of Reverberant Sound Fields," *Journal of the Acoustical Society of America*, Vol. 43, No. 6, 1968, pp. 1433–1436.

[3] Chu, W. T., "Eigenmode Analysis of the Interference Patterns in Reverberant Sound Fields," *Journal of the Acoustical Society of America*, Vol. 68, No. 1, 1980, pp. 184–190.

[4] Zeng, L. J., "The Sound Distribution in a Rectangular Reverberation Chamber," *Journal of the Acoustical Society of America*, Vol. 92, No. 1, 1992, pp. 600–603.

[5] Jones, D. S., "Diffraction Theory: a Brief Introductory Review," *Journal of Sound and Vibration*, Vol. 20, No. 1, 1972, pp. 71–78.

[6] Cassot, F., "Contribution á l'étude de la diffraction par un écran mince," *Acoustica*, Vol. 34, No. 1, 1975, pp. 64–71.

[7] Huang, C. J., and Chwang, A. T., "Diffraction of Acoustic Waves by Rigid Plane Baffles," *Journal of the Acoustical Society of America*, Vol. 95, No. 2, 1994, pp. 668–680.

[8] Huang, C. J., and Chwang, A. T., "Diffraction of Acoustic Waves by a Ring Aperture in a Baffle of Arbitrary Impedance," Iowa Inst. of Hydraulic Research, IIHR Rept. 350, Univ. of Iowa, 1991.

[9] Bouwkamp, C. J., "Diffraction Theory," *Report of Progress in Physics*, Vol. 17, 1954, pp. 35–100.

[10] Filippi, P., "Layer Potential and Acoustic Diffraction," *Journal of Sound and Vibration*, Vol. 54, 1977, pp. 473–500.

[11] Clarkson, B. L., Cummins, R. J., Eaton, D. C. G., and Vessaz, J. P., "Prediction of High-Frequency Structural Vibrations Using Statistical Energy Analysis (SEA)," *European Space Agency Journal*, Vol. 5, No. 2, 1981, pp. 137–152.

[12] Troclet, B., Trong, T. D., and Vidal, C., "Prediction of the High-Frequency Response of Satellites to Diffuse Acoustic Environments," *Proceedings of the Conference Spacecraft Structures*, Centre National d'Études Spatiales, Toulouse, France, 1985, pp. 145–150.

[13] Borello, G., "Acoustic Intensity Techniques Applied to Parameter Identification of Noise Under a Fairing Through a SEA Model," *Proceedings of the 28th Structures, Structural Dynamics, and Materials Conference* (Monterey, CA), AIAA, Washington, DC, 1987, pp. 844–849.

[14] Defosse, H., and Mercier, F., "Acoustic Response Analysis of Large Light Space Structures," *Proceedings of the 40th Conference International Astronautical Federation*, Malaga, Spain, 1989, pp. 1–7.

[15] Morand, H. J.-P., and Ohayon, R., *Intéraction fluide-structure*, Édition Masson, Paris.

[16] Mercier, F., Gangloff, D., and Mamode, A., "Acoustic Response Analysis of Large Space Structures," *7th International Modal Analysis Conference* (Las Vegas, NV) 1989, pp. 1611–1615.

[17] Everstine, G. C., and Henderson, F. M., "Coupled Finite Element/Boundary Element Approach for Fluid-Structure Interaction," *Journal of the Acoustical Society of America*, Vol. 87, No. 5, 1990, pp. 1938–1947.

[18] Hamdi, M. A., "Formulation variationnelle par équations intégrales pour le calcul de champs acoustiques linéaires proches et lointains," Ph.D. Thesis, Université de Technologie de Compiégne, 1982.

[19] Ouellet, D., Guyader, J. L., and Nicolas, J., "Sound Field in a Rectangular Cavity in the Presence of a Thin, Flexible Obstacle by the Integral Equation Method," *Journal of the Acoustical Society of America*, Vol. 89, No. 5, 1991, pp. 2131–2139.

[20] Beslin, O., "Rayonnement et transparence acoustique des plaques trouées," Ph.D. Science Thesis, Institut National des Sciences Appliquées de Lyon, 1993.

[21] Jackson, J. D., *Classical Electrodynamics*, 2nd ed., Wiley, New York, 1975.

[22] Bruneau, M., *Introduction aux théories de l'acoustique*," Université du Maine Éditeur, Le Mans, France, 1983.

[23] Pierce, A. D., *Acoustics: An Introduction to Its Physical Principles and Applications*, McGraw–Hill, New York, 1981.